Mesostructural control of non-silica-based hybrid mesoporous film composed of aluminium ethylenediphosphonate using triblock copolymer and their TEM observation

Tatsuo Kimura* and Kazumi Kato

Received (in Montpellier, France) 14th March 2007, Accepted 24th April 2007
First published as an Advance Article on the web 15th May 2007
DOI: 10.1039/b703841k

A mixed solution of ethanol and water containing $EO_{80}PO_{30}EO_{80}$ was combined with a solution prepared by the reaction between $(HO)_2OPC_2H_4O(OH)_2$ and $AlCl_3$ in ethanol–water in order to obtain clear precursor solutions for the synthesis of ordered mesoporous aluminium organophosphonate (AOP) films with high transparency. The amount of $EO_{80}PO_{30}EO_{80}$ in the precursor solution strongly influenced the mesostructural ordering of the AOP films, which was mainly investigated through TEM observations. Ordered mesoporous AOP films can be obtained and their high porosity was proved by direct N_2 adsorption–desorption measurement. High adsorption capacity of acetaldehyde molecules over such films was also confirmed.

1 Introduction

Fabrication of surfactant templated mesoporous materials is important for their application in the formation of ordered mesoporous films for optical, electronic and photonic devices[1–4] in combination with the compositional variation of pore walls.[5–8] In recent years, triblock copolymer templating has been developed and expanded the possibility to synthesize non-silica-based mesoporous films.[1–4] A wide variety of non-silica-based mesoporous oxide films such as TiO_2, ZrO_2, Nb_2O_5, CeO_2, V_2O_5, WO_3, ZnO and SnO_2, including phosphates such as TiPO and AlPO have been synthesized and several research groups have attempted to investigate their unique properties due to the inorganic frameworks surrounding ordered mesopores.[9–13]

Highly ordered mesostructured films are produced during evaporation of solvents which induces the self-assembly of surfactant molecules. Accordingly, reactivity of inorganic species attached with the surfactant molecules strongly influences the ordering and transparency of the mesostructured films and its control is necessary for the formation of high-quality mesoporous films because non-silica-based inorganic species are condensed much faster than silicate species. Besides, as in the case of silica-based materials,[14–16] organic modification of TiO_2, ZrO_2 and AlPO is also started by using organosilanes and related compounds.[17–20] Especially, facile surface modification of phosphate-based materials is possible by using monophosphonic acids and the porosity and the number of organic groups are controllable according to the proportion of the monophosphonic acids to phosphoric acid.[21–25] In silica-based mesoporous materials, photochemical and electrochemical properties are imparted to the frameworks by incorporating organic groups in the pore walls; such hybrid frameworks are constructed through the reaction of bridged silsesquioxanes.[15,16] However, it is difficult to synthesize similar non-silica-based hybrid mesoporous films with integral inorganic–organic frameworks because of the lack of appropriate precursors such as organically bridged metal alkoxides. There have been only a few reports on the synthesis of non-silica-based hybrid mesoporous materials without surfactants through the preparation of bridged organotin compounds.[26,27]

A synthetic strategy of non-silica-based hybrid mesoporous materials by using organically bridged diphosphonic acids has been proposed.[28] The actual synthesis of 2-D hexagonal mesoporous aluminium organophosphonates (AOPs) by using alkylene diphosphonic acids proved the suitability of the synthetic strategy.[28–30] In accordance with the strategy, the use of diphosphonic acids is applicable to further compositional variation of non-silica-based mesoporous hybrids.[28–32] It is also found that transparent AOP films can be prepared through the reaction of aluminium chloride and ethylenediphosphonic acid in the presence of $EO_nPO_mEO_n$-type triblock copolymer.[33] The resulting films contain wormhole-like mesopores exposed at the film surfaces as confirmed by TEM, high-resolution SEM, and in-plane XRD.

In the present study, the synthesis of mesoporous AOP films is presented as a candidate for the fabrication of non-silica-based hybrid materials using $EO_nPO_mEO_n$-type triblock copolymer. Mesostructural control of the AOP films was mainly investigated by TEM of the films prepared from clear precursor solutions containing different amounts of the triblock copolymer. The preparative method of the clear precursor solution through the reaction of ethylenediphosphonic acid with aluminium chloride was modified to obtain ordered mesoporous AOP films. On the basis of reactivities between other metal species (chlorides, alkoxides, *etc.*) and diphosphonic acids and/or diphosphonates, the method is potentially applicable to the synthesis of a wide variety of metal phosphonate-based mesoporous films.

Advanced Manufacturing Research Institute, National Institute of Advanced Industrial Science and Technology (AIST), Shimoshidami, Moriyama-ku, Nagoya, 463–8560, Japan. E-mail: t-kimura@aist.go.jp

2 Experimental

2.1 Materials

Pluronic F68 ($EO_{80}PO_{30}EO_{80}$) was obtained from Sigma-Aldrich and used as $EO_nPO_mEO_n$-type triblock copolymer. Ethylenediphosphonic acid ($(HO)_2OPC_2H_4PO(OH)_2$) was purchased from AZmax Co. Ltd. Aluminium chloride ($AlCl_3$) and ethanol were obtained from Wako Chemical Co.

2.2 Synthesis of AOP films using triblock copolymer

In a typical synthesis, 1.6 g of $EO_{80}PO_{30}EO_{80}$ was dissolved in a mixed solvent of ethanol (10 mL) and water (1 mL). Separately, $(HO)_2OPC_2H_4PO(OH)_2$ (0.96 g) was dissolved in another mixed solution of ethanol (10 mL) and water (1 mL). Then, $AlCl_3$ (0.67 g) was added to the clear solution under vigorous stirring in order to react with the diphosphonic acid beforehand (Al : 2P = 1 : 1). After reaction for 15 min, the latter solution was added to the surfactant solution under stirring and the stirring was maintained for another 2 h. The resultant clear solution was spin-coated at a spinning rate of 3000 rpm. Similar clear precursor solutions containing different amounts of $EO_{80}PO_{30}EO_{80}$ (0.8–3.2 g) were also prepared. Air-dried transparent films were heated up to 250 °C with a heating rate of 1 °C min^{-1} and kept for 1 h at this temperature in nitrogen flow, followed by calcination at this temperature for 2 h in oxygen flow. Complete retention of ethylene groups in the aluminium organophosphonate (AOP) framework after calcination at 250 °C has already been reported in our previous paper.[33]

2.3 Characterization

X-Ray diffraction (XRD) patterns of the films on glass substrates were obtained by using a Rigaku RINT 2100 diffractometer with monochromated Fe Kα radiation. Transmission electron microscopic (TEM) images, which were obtained from corresponding samples scraped off from the glass substrates, were taken using a JEOL JEM 2010 (200 kV). N_2 adsorption–desorption data were directly collected from the film coated on Si(100) substrate by using a Quantachrome Autosorb-1 at 77 K. The film was preheated at 110 °C for 6 h under vacuum. Specific surface area and average pore diameter were calculated by the BET method[34] and the density functional theory (DFT) method based on the data on carbon, respectively. Adsorption measurement of acetaldehyde was conducted at room temperature (at around 27 °C) in a closed glass line with a total volume of 372.1 cm^3. The initial concentration of acetaldehyde vapor was 10 ppm and 4.2 × 10^{-3} cm^3 of the dried films were placed in the closed line.

3 Results and discussion

3.1 Synthesis of ordered mesoporous AOP films

The XRD patterns of calcined AOP films prepared from clear precursor solutions containing different amounts of $EO_{80}PO_{30}EO_{80}$ (0.8–1.6 g) are shown in Fig. 1. In the calcined AOP film prepared using 0.8 g of $EO_{80}PO_{30}EO_{80}$, the XRD pattern showed a broad peak with a *d*-spacing of 5.5 nm. The XRD pattern of the calcined AOP film prepared in the presence of 1.2 g of $EO_{80}PO_{30}EO_{80}$ also showed a broad peak with a *d*-spacing of 5.9 nm. The representative TEM image of the calcined AOP film is shown in Fig. 2. Disordered mesopores and very small domains of ordered structure were observed over the entire film. The mesostructural ordering was gradually improved with an increase in the amount of $EO_{80}PO_{30}EO_{80}$ in the precursor solutions. A sharp peak was observed in the XRD pattern of the calcined AOP film prepared using 1.6 g of $EO_{80}PO_{30}EO_{80}$ and the *d*-spacing was 6.9 nm, revealing that the reactivity of the resultant solution was improved for obtaining ordered mesoporous AOP film, possibly with 3-D hexagonal structure, which is suggested from the TEM observation. The TEM images of the calcined AOP film are shown in Fig. 3. Hexagonally arranged mesopores were observed by the TEM observation (top image in Fig. 3). Different images were also taken as shown in bottom images in Fig. 3. However, there were no striped patterns showing clearly separated pore and wall regions that are typically observed for 2-D hexagonal mesophase silicates.[35–37] Small striped images with some directions were observed with unclear contrast in the same film. The result is possibly related to the fact that small domains of

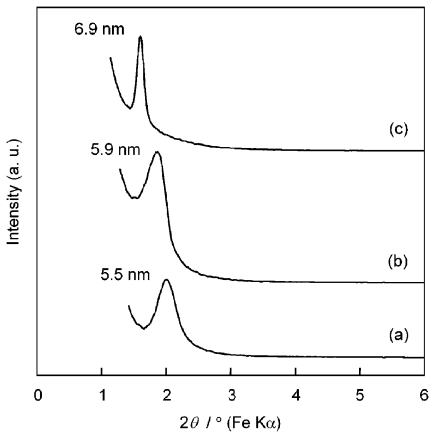

Fig. 1 XRD patterns of calcined (at 250 °C) AOP films prepared using (a) 0.8 g, (b) 1.2 g and (c) 1.6 g of $EO_{80}PO_{30}EO_{80}$.

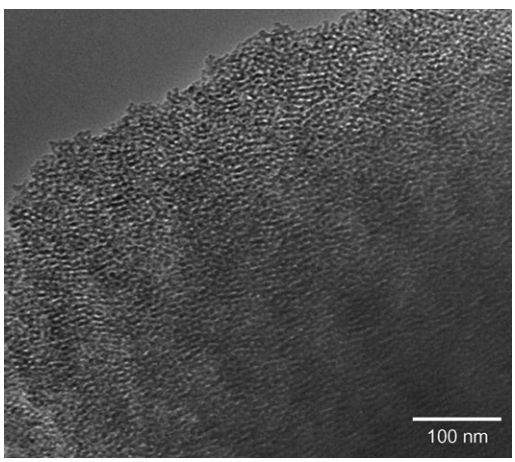

Fig. 2 Representative TEM image of a calcined (at 250 °C) AOP film prepared using 1.2 g of $EO_{80}PO_{30}EO_{80}$.

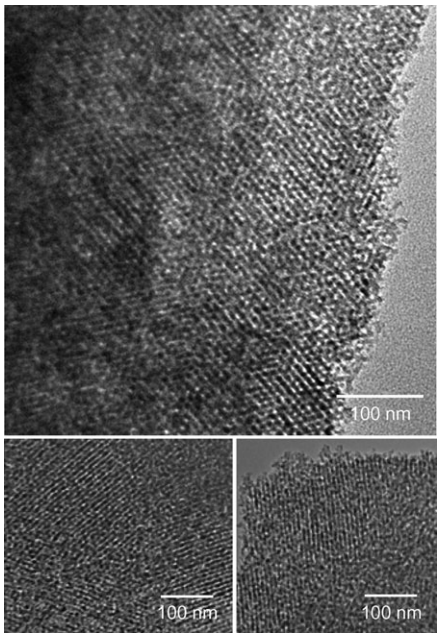

Fig. 3 TEM images of a calcined (at 250 °C) AOP film prepared using 1.6 g of $EO_{80}PO_{30}EO_{80}$.

cage-type mesoporous structures such as 3-D hexagonal structures are not accumulated over the whole calcined film. The film showed substantial shrinkage on heating as confirmed by XRD in Fig. 4. A sharp peak with a *d*-spacing of 9.1 nm with higher order diffraction was observed for the XRD pattern of the as-synthesized AOP film. The position of the peak was considerably shifted to higher diffraction angles during the drying process at 50 °C and subsequent calcination process at 250 °C. In general, mesostructured films are shrunk perpendicular to the substrates, largely by calcination, but do not contract parallel to the substrates so drastically because of the presence of covalent bonds at the interface between the film and the substrate.[38–40] Thus, highly ordered images would not be observed through the TEM observations.

3.2 Investigation on mesostructural ordering and porosity of AOP films

In silica-based materials prepared using $EO_nPO_mEO_n$-type triblock copolymers, the EO : PO ratio and molecular weight of the triblock copolymers is quite important for the mesophase control.[41–43] Initially, it was reported that the use of triblock copolymers with low EO : PO ratios leads to the formation of lamellar phases and higher ratios promote the formation of cubic phases. The use of $EO_{80}PO_{30}EO_{80}$ leads to the preferential formation of cubic $Ia\bar{3}d$ phases and cage-type ones with $Fm\bar{3}m$ and $Pm\bar{3}m$ structures because of the high EO : PO ratio.[44,45] On the basis of the results on the synthesis using some $EO_nPO_mEO_n$-type triblock copolymers, it can be summarized that lower and higher EO/(EO + PO) ratios are found to favor the formation of hexagonal and cubic mesophases, respectively. In the case of AOP, 2-D hexagonal phases are preferentially obtained using $EO_nPO_mEO_n$-type triblock copolymers in spite of the molecules structures.[30] This would be related to the fact that the AOP frameworks are not condensed adequately and then the geometrical packing of the $EO_nPO_mEO_n$ molecules containing inorganic species attached with EO moieties could be different from those of $EO_nPO_mEO_n$-silica mesophases.

The N_2 adsorption–desorption isotherm and pore size distribution of the calcined AOP film prepared using 1.6 g of $EO_{80}PO_{30}EO_{80}$ was directly measured by using the corresponding film on Si substrate (*ca.* 95.1 cm^2) with a thickness of 0.58 ± 0.05 μm. The isotherm is shown in Fig. 5. This type IV isotherm measured is typically observed for ordered mesoporous materials. A hysteresis loop was also observed in the isotherm, which is usually confirmed in those observed for materials with larger mesopores (such as SBA-15) or with windows of cage-type mesopores (such as SBA-16).[46–55] The shape of the isotherm is not analogous to that generally observed for SBA-15 with one-dimensional large mesopores.[41] In SBA-15, the slope due to capillary condensation in the adsorption branch is similar to that in the desorption blanch. However, the slope in the desorption branch, possibly due to the pore blocking of cage-type mesopores, is not so large

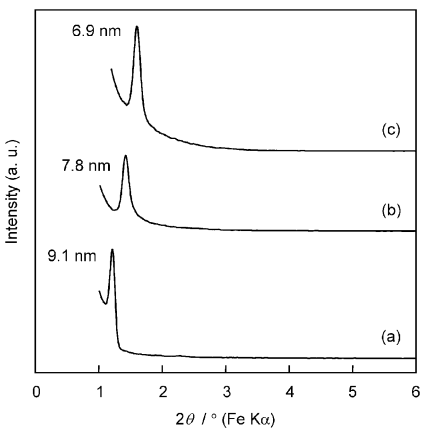

Fig. 4 XRD patterns of (a) as-synthesized AOP film prepared using 1.6 g of $EO_{80}PO_{30}EO_{80}$, the AOP film (b) dried at 50 °C and (c) calcined at 250 °CH.

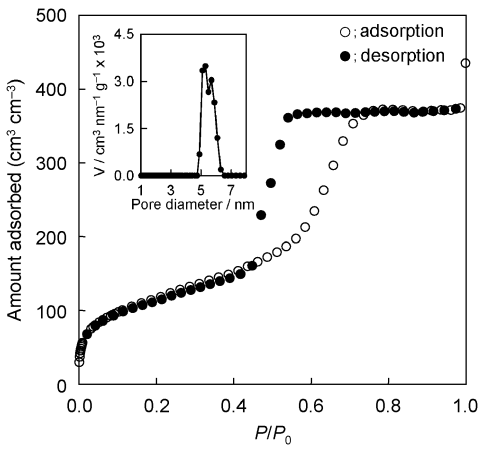

Fig. 5 N_2 adsorption–desorption isotherm and pore size distribution of calcined (at 250 °C) AOP film prepared using 1.6 g of $EO_{80}PO_{30}EO_{80}$.

compared with those observed for cage-type mesoporous materials such as SBA-16 and FDU-12.[46–55] Therefore, it is considered that cage-type mesopores are not connected over the whole films so regularly, this being in good agreement with the result by the TEM observation (see Fig. 3). Although the mass of the film cannot be measured correctly and the density of the AOP framework is unclear, the BET surface area and the pore volume were roughly estimated to be approximately 460 m^2 cm^{-3} and 0.72 cm^3 cm^{-3}, respectively. The average pore diameter calculated using adsorption data was *ca.* 5.4 nm.

Mesoporous materials with aluminophosphate-like units are reported to be useful for removing harmful organic molecules such as acetaldehyde.[29] Thus, direct adsorption measurement of acetaldehyde on an AOP film prepared using 1.6 g of $EO_{80}PO_{30}EO_{80}$ was investigated in a closed vessel. The pressure due to acetaldehyde gas in the vessel (initial; 4.8 mmHg, 10 ppm) became constant within 10 s (final; 4.2 mmHg). The result suggests that acetaldehyde molecules are adsorbed quickly on the film and *ca.* 0.5 mg of the molecules can be eliminated by using the films with a total volume of 4.2×10^{-3} cm^3 (0.12 g of acetaldehyde per film volume of 1 cm^3). It is considered that highly ordered AOP films with active surfaces is applicable to sensing devices to detect or remove harmful organic molecules.

3.3 Influence of the amount of the triblock copolymer in the precursor solution on mesostructural ordering of AOP film

AOP films were also synthesized when clear precursor solutions containing larger amounts of $EO_{80}PO_{30}EO_{80}$ (2.0–3.2 g) were used. The XRD patterns are shown in Fig. 6. In the case of the calcined AOP film prepared in the presence of 2.0 g of $EO_{80}PO_{30}EO_{80}$, the peak observed in low diffraction angles was broadened, though the *d*-spacing (6.9 nm) was similar to that observed for the calcined AOP film prepared using 1.6 g of $EO_{80}PO_{30}EO_{80}$. When further $EO_{80}PO_{30}EO_{80}$ was added under the same conditions, the mesoporous films became impure and finally no mesostructural ordering was observed by TEM. Representative TEM images of calcined AOP films prepared using different amounts of $EO_{80}PO_{30}EO_{80}$ (2.0–3.2 g) are shown in Fig. 7. The TEM image of the film prepared in the presence of 2.0 g of

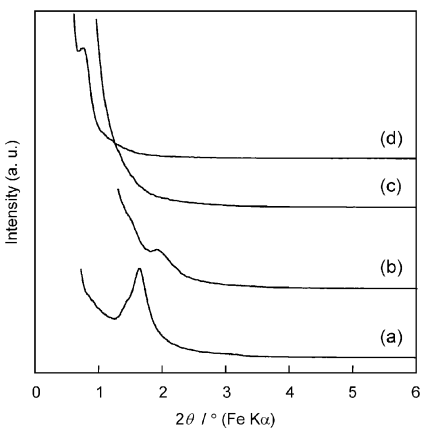

Fig. 6 XRD patterns of calcined (at 250 °C) AOP films prepared using (a) 2.0 g, (b) 2.4 g, (c) 2.8 g and (d) 3.2 g of $EO_{80}PO_{30}EO_{80}$.

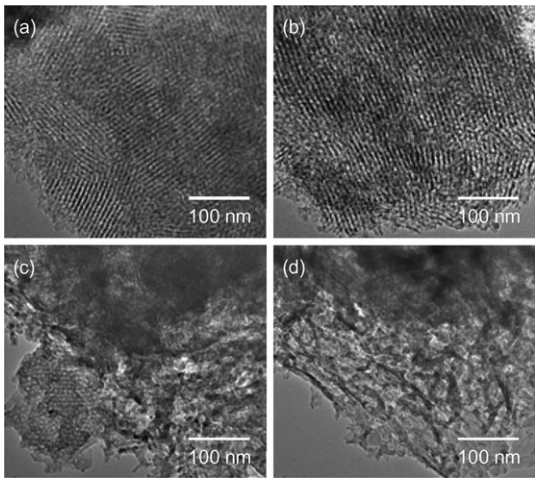

Fig. 7 Representative TEM images of calcined (at 250 °C) AOP film prepared using (a) 2.0 g, (b) 2.4 g, (c) 2.8 g and (d) 3.2 g of $EO_{80}PO_{30}EO_{80}$.

$EO_{80}PO_{30}EO_{80}$ showed the presence of periodic structure but the periodicity in some directions does not have a long-range ordering (as similarly occasionally observed for the film prepared using 1.6 g of $EO_{80}PO_{30}EO_{80}$) (see bottom images in Fig. 3). The mesostructural ordering was gradually decreased with an increase in the added amount of $EO_{80}PO_{30}EO_{80}$, leading to the formation of other phases that are not defined by assemblies of $EO_{80}PO_{30}EO_{80}$. Much larger pores were formed over the entire films and would be formed through a phase separation by the presence of excess $EO_{80}PO_{30}EO_{80}$. Including the above data on the AOP films prepared using 0.8–1.6 g of $EO_{80}PO_{30}EO_{80}$, the variation in the mesostructural ordering of the AOP films can be summarized as a function of the amount of $EO_{80}PO_{30}EO_{80}$. With an increase in the amount of $EO_{80}PO_{30}EO_{80}$ in the precursor solutions, mesostructural ordering is increased and cage-type mesopores possibly form in the AOP film according to the molecular structure of $EO_{80}PO_{30}EO_{80}$. Further increase of $EO_{80}PO_{30}EO_{80}$ in the precursor solutions leads to the distortion of the mesostructural ordering, and finally a number of intercrystalline spaces are formed containing excess $EO_{80}PO_{30}EO_{80}$ over the whole films.

4 Conclusions

Ordered mesoporous AOP films with a unique property to adsorb aldehydes can be successfully prepared by the reaction of $(HO)_2PC_2H_4O(OH)_2$ and $AlCl_3$ in ethanol–water containing $EO_nPO_mEO_n$-type triblock copolymer. The mesostructural ordering is strongly influenced by the amount of the triblock copolymer contained in the precursor solution. The synthetic method should be applicable for the development of synthetic procedures of other metal phosphonate-based mesoporous films with integrated inorganic–organic hybrid frameworks, promising the intentional design of hybrid frameworks to afford versatile mesoporous films.

Acknowledgements

This work was partly supported by the Core Research for Evolutional Science and Technology (CREST), Japan Science and Technology Agency (JST), Japan. The A3 Foresight Program "Synthesis and Structural Resolution of Novel Mesoporous Materials" supported by the Japan Society for Promotion of Science (JSPS) is also acknowledged.

References

1 C. Yu, B. Tian and D. Zhao, *Curr. Opin. Solid State Mater. Sci.*, 2003, **7**, 191.
2 B. Tian, X. Liu, B. Tu, C. Yu, J. Fan, L. Wang, S. Xie, G. D. Stucky and D. Zhao, *Nat. Mater.*, 2003, **2**, 159.
3 Y. Wan, H. Yang and D. Zhao, *Acc. Chem. Res.*, 2006, **39**, 423.
4 Y. Wan, Y. Shia and D. Zhao, *Chem. Commun.*, 2007, 897.
5 P. Behrens, *Angew. Chem., Int. Ed. Engl.*, 1996, **35**, 515.
6 A. Sayari and P. Liu, *Microporous Mater.*, 1997, **12**, 149.
7 F. Schüth, *Chem. Mater.*, 2001, **13**, 3184.
8 T. Kimura, *Microporous Mesoporous Mater.*, 2005, **77**, 97.
9 E. Stathatos, T. Petrova and P. Lianos, *Langmuir*, 2001, **17**, 5025.
10 J. C. Yu, X. Wang and X. Fu, *Chem. Mater.*, 2004, **16**, 1523.
11 K. L. Frindell, J. Tang, J. H. Harreld and G. D. Stucky, *Chem. Mater.*, 2004, **16**, 3524.
12 I. S. Nandhakumar, T. Gabriel, X. Li, G. S. Attard, M. Markham, D. C. Smith and J. J. Baumberg, *Chem. Commun.*, 2004, 1374.
13 M. Zukalova, A. Zukal, L. Kavan, M. K. Nazeeruddin, P. Liska and M. Gratzel, *Nano Lett.*, 2005, **5**, 1789.
14 J. H. Clark and D. J. Macquarrie, *Chem. Commun.*, 1999, 853.
15 A. Sayari and S. Hamoudi, *Chem. Mater.*, 2001, **13**, 3168.
16 F. Hoffmann, M. Cornelius, J. Morell and M. Fröba, *Angew. Chem., Int. Ed.*, 2006, **45**, 3216.
17 T. Kimura, *Chem. Lett.*, 2002, **31**, 770.
18 T. Kimura, *J. Mater. Chem.*, 2003, **13**, 3072.
19 P. C. Angelomé, S. Aldabe-Bilmes, M. E. Calvo, E. L. Crepaldi, D. Grosso, C. Sanchez and G. J. A. A. Soler-Illia, *New J. Chem.*, 2005, **29**, 59.
20 K. Sarkar, S. C. Laha and A. Bhaumik, *J. Mater. Chem.*, 2006, **16**, 2439.
21 J. E. Haskouri, C. Guillem, J. Latorre, A. Beltrán, D. Beltrán and P. Amorós, *Eur. J. Inorg. Chem.*, 2004, 1804.
22 J. E. Haskouri, C. Guillem, J. Latorre, A. Beltrán, D. Beltrán and P. Amorós, *Chem. Mater.*, 2004, **16**, 4359.
23 X. Shi, J. Yang and Q. H. Yang, *Eur. J. Inorg. Chem.*, 2006, 1936.
24 N. K. Mal, M. Fujiwara and M. Matsukata, *Chem. Commun.*, 2005, 5199.
25 N. K. Mal, A. Bhaumik, M. Fujiwara and M. Matsukata, *Microporous Mesoporous Mater.*, 2006, **93**, 40.
26 H. Elhamzaoui, B. Jousseaume, H. Riague, T. Toupance, P. Dieudonne, C. Zakri, M. Maugey and H. Allouchi, *J. Am. Chem. Soc.*, 2004, **126**, 8130.
27 H. Elhamzaoui, T. Toupance, M. Maugey, C. Zakri and B. Jousseaume, *Langmuir*, 2007, **23**, 785.
28 T. Kimura, *Chem. Mater.*, 2003, **15**, 3742.
29 T. Kimura, *Chem. Mater.*, 2005, **17**, 337.
30 T. Kimura, *Chem. Mater.*, 2005, **17**, 5521.
31 T. Kimura and K. Kato, *J. Mater. Chem.*, 2007, **17**, 559.
32 T. Kimura and K. Kato, *Microporous Mesoporous Mater.*, 2007, **101**, 207.
33 T. Kimura and K. Kato, *Stud. Surf. Sci. Catal.*, in press.
34 K. S. W. Sing, D. H. Everett, R. A. W. Haul, L. Moscou, R. A. Pierotti, J. Rouquerol and T. Siemieniewska, *Pure Appl. Chem.*, 1985, **57**, 603.
35 C.-Y. Chen, S.-Q. Xiao and M. E. Davis, *Microporous Mater.*, 1995, **4**, 1.
36 J. Fan, C. Yu, L. Wang, B. Tu, D. Zhao, Y. Sakamoto and O. Terasaki, *J. Am. Chem. Soc.*, 2001, **123**, 12113.
37 M. Kruk, M. Jaroniec, Y. Sakamoto, O. Terasaki, R. Ryoo and C. H. Ko, *J. Phys. Chem. B*, 2000, **104**, 292.
38 H. Miyata, Y. Kawashima, M. Itoh and M. Watanabe, *Chem. Mater.*, 2005, **17**, 5323.
39 M. P. Tate, B. W. Eggiman, J. D. Kowalski and H. W. Hillhouse, *Langmuir*, 2005, **21**, 10112.
40 C.-W. Wu, T. Ohsuna, M. Kuwabara and K. Kuroda, *J. Am. Chem. Soc.*, 2006, **128**, 4544.
41 D. Zhao, J. Feng, Q. Huo, N. Melosh, G. H. Fredrickson, B. F. Chmelka and G. D. Stucky, *Science*, 1998, **279**, 548.
42 D. Zhao, Q. Huo, J. Feng, B. F. Chmelka and G. D. Stucky, *J. Am. Chem. Soc.*, 1998, **120**, 6024.
43 P. Kipkemboi, A. Fogden, V. Alfredsson and K. Flodstrom, *Langmuir*, 2001, **17**, 5398.
44 S. A. El-Safty, F. Mizukami and T. Hanaoka, *J. Phys. Chem. B*, 2005, **109**, 9255.
45 S. A. El-Safty, T. Hanaoka and F. Mizukami, *Chem. Mater.*, 2005, **17**, 3137.
46 P. I. Ravikovitch and A. V. Neimark, *Langmuir*, 2002, **18**, 9830.
47 A. Vishnyakov and A. V. Neimark, *Langmuir*, 2003, **19**, 3240.
48 K. Morishige, N. Tateishi and S. Fukuma, *J. Phys. Chem. B*, 2003, **107**, 5177.
49 K. Morishige, H. Uematsu and N. Tateishi, *J. Phys. Chem. B*, 2004, **108**, 7241.
50 K. Morishige, M. Tateishi, F. Hirose and K. Aramaki, *Langmuir*, 2006, **22**, 9220.
51 K. Morishige and N. Tarui, *J. Phys. Chem. C*, 2007, **111**, 280.
52 V. Antochshuk, M. Kruk and M. Jaroniec, *J. Phys. Chem. B*, 2003, **107**, 11900.
53 T.-W. Kim, R. Ryoo, M. Kruk, K. P. Gierszal, M. Jaroniec, S. Kamiya and O. Terasaki, *J. Phys. Chem. B*, 2004, **108**, 11480.
54 M. Kruk, E. B. Celer, J. R. Matos, S. Pikus and M. Jaroniec, *J. Phys. Chem. B*, 2005, **109**, 3838.
55 T. Yu, H. Zhang, X. Yan, Z. Chen, X. Zou, P. Oleynikov and D. Zhao, *J. Phys. Chem. B*, 2006, **110**, 21467.

